41th "Jaszowiec" International School and Conference on the Physics of Semiconductors, Krynica-Zdrój 2012

XPS and Raman Characterizations of $Zn_{1-x}Cd_xO$ Films Grown at the Different Growth Conditions

I. Shtepliuk[a,*], O. Khyzhun[a], G. Lashkarev[a], V. Khomyak[b] and V. Lazorenko[a]

[a]I. Frantsevich Institute for Problems of Material Science, NASU, 03680, Kiev, Ukraine

[b]Chernivtsi National University, 58012, Chernivtsi, Ukraine

X-ray photoelectron spectroscopy was employed to characterize the surface chemistry and electronic properties of the $Zn_{1-x}Cd_xO$ semiconductor systems obtained at the different growth conditions. The effect of the growth conditions on the core and valence band spectra as well as room-temperature photoluminescence of the $Zn_{1-x}Cd_xO$ films was investigated and discussed. Behavior of the mX-ray photoelectron spectroscopy peaks indicated an increase of the cadmium and a depletion of the oxygen concentrations upon changing the Ar/O_2 gas ratio and dc power.

PACS: 78.55.Et, 78.67.Bf

1. Introduction

ZnO and its ternary alloys $Zn_{1-x}Cd_xO$ are important semiconductor materials that may be used in solar cells [1], light-emitting diodes [2], and other optoelectronic devices [3]. Due to their chemical and structural compatibility they may be also utilized for growing heterostructures of $ZnO/Zn_{1-x}Cd_xO$ emitted in the visible range [4]. The incorporation of Cd ions into ZnO makes the lattice of $Zn_{1-x}Cd_xO$ tunable [5], by adjusting the Zn/Cd ratio, hence, a better lattice-matched substrate for the growth of the ZnO epitaxial layer may be expected [6]. Furthermore, the designable semiconductor band gap is obviously helpful for controlling the resistivity as well as the valence and conduction band alignment at the semiconductor interface [7]. The control and monitoring of the Cd concentration, especially at the surface, is crucial for obtaining a $Zn_{1-x}Cd_xO$ alloy with the required lattice parameter for matching ZnO. Also, it is an important consideration for its use as an emitter material. Furthermore, it is important to characterize and control the surface electronic structure and chemical composition of the substrate for the epitaxial layer growth and the device performance [8].

In spite of the remarkable interest, which is related to the specific properties of the $Zn_{1-x}Cd_xO$ ternary alloys, no studies are focused mostly on the correlation of the electronic structure and phonon spectrum with deposition parameters. Thus, achieving the control over electronic and vibrational properties of the $Zn_{1-x}Cd_xO$ alloy is a challenging task. In this paper, we report the characterization of $Zn_{1-x}Cd_xO$ ternary alloys grown by means of the dc magnetron sputtering technique. The influence of the gas ratio of Ar/O_2 and dc power on the surface chemistry, valence band features as well as the phonon and photoluminescence (PL) properties of the ternary alloys is investigated and presented.

2. Experimental details

The $Zn_{1-x}Cd_xO$ films were grown by the dc magnetron sputtering on the sapphire c-Al_2O_3 substrates at the temperature of 250 °C. A disc of 90%zinc–10%cadmium alloy (100 mm in a diameter) with a purity of 99.99% was used as a target. High purity argon and oxygen were used as the sputtering and the reactive gas, respectively. The target-to-substrate distance was about 40 mm. The chamber was pumped to a base pressure of 1×10^{-4} Pa before deposition. The films were grown in the ambient with the Ar/O_2 ratio ranging from 2:1 to 4:1. The dc power was changed from 100 to 150 W. The X-ray photoelectron spectroscopy (XPS) valence-band and the core-level spectra were measured by means of the UHV--Analysis–System assembled by the SPECS (Germany). The system is equipped with a PHOIBOS 150 hemispherical analyzer. A base pressure in the sublimation ion--pumped chamber of the system was less than 9×10^{-8} Pa during the present experiments. The Mg K_α radiation ($E = 1253.6$ eV) was used as a source of XPS spectra excitation. The XPS spectra were measured at the constant pass energy of 25 eV. The binding energy (BE) of 84.00 ± 0.05 eV of the XPS Au $4f_{7/2}$ core-level spectrum was used as a reference. Deviations of error in all binding energy (BE) values are within ± 0.05 eV. Room temperature (RT) non-resonant Raman spectra were measured with a Jobin–Yvon T64000 spectrometer equipped with a CCD detector, in a back scattering geometry, using an Ar^+/Kr^+ ion laser (514.5 nm) with an incident power of 12 mW. Resonant Raman scattering (RRS) and PL spec-

* corresponding author; e-mail: shtepliuk_1987@ukr.net

tra were measured using the 325 nm excitation line of a He–Cd laser.

3. Results and discussion

In order to elucidate the nature of the changes in composition of the $Zn_{1-x}Cd_xO$ surface under influence of the growth conditions, XPS spectra were obtained for all samples. Figure 1 gives the wide-scan XPS spectra of $Zn_{1-x}Cd_xO$ samples grown at the different growth conditions. Zn, O, and Cd elements were detected in the samples. All presented samples exhibited the expected adsorption of adventitious carbon. It should be noted that this adsorbent is primarily hydrocarbons whose binding energy should be $\approx$ 284.6 eV and can thus be used for referencing. No other species were detectable above the noise level of the spectra. The various spectra were compared in order to determine the chemical interactions that occurred upon changing the Ar/O_2 gas ratio and dc power (Fig. 1a–c). The XPS spectral fitting parameters (binding energy, BE; full widths at half-maximum, FWHM; integral area, A) for the samples are given in Table I.

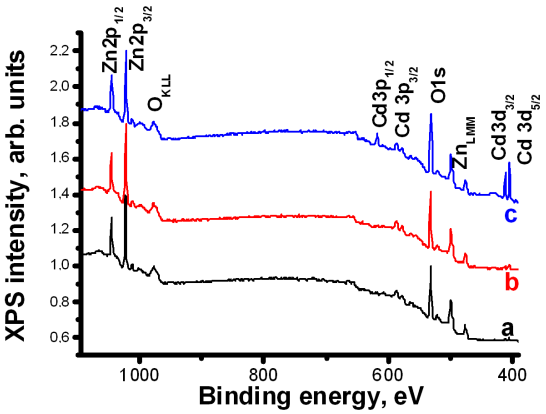

Fig. 1. XPS survey spectra of the $Zn_{1-x}Cd_xO$ ternary alloys deposited at the different growth conditions: (a) Ar/O_2 gas ratio of 2:1, dc power of 100 W, (b) 4:1, 100 W, (c) 2:1, 150 W.

TABLE I

Zn ($2p$ 3/2), Cd ($3d$ 3/2) and O ($1s$) XPS spectral fitting parameters (binding energy, BE; full widths at half-maximum, FWHM; integral area, A) for the $Zn_{1-x}Cd_xO$ ternary alloys grown at the different growth conditions.

Conditions	XPS peaks								
	O $1s$			Zn $2p$ 3/2			Cd $3d$ 5/2		
	BE [eV]	FWHM [eV]	A	BE [eV]	FWHM [eV]	A	BE [eV]	FWHM [eV]	A
2:1, 100	531.758	2.630	0.811	1022.070	2.725	1.252	405.398	2.340	0.049
4:1, 100	531.776	2.528	0.871	1022.002	2.731	1.282	405.211	2.171	0.053
2:1, 150	531.523	2.475	0.945	1021.753	2.585	1.087	405.128	2.259	0.493

The XPS Zn $2p_{3/2}$ peak corresponding to Zn^{2+} ions, observed at about 1022.07 eV for the sample grown at the gas ratio of 2:1, shifted to the lower binding energy of 1022.00 eV when the gas ratio changes from 2:1 to 4:1. This shift in binding energy may be due to enlargement of the partial substitution of Zn^{2+} in $Zn_{1-x}Cd_xO$ lattice by the Cd^{2+} ions. The enhancement of the site-to-site substitution may be associated with the fact that more cadmium ions are incorporated into the zinc oxide matrix when the gas ratio is increased. The different Ar/O_2 gas ratios correspond to the different saturated vapor pressures and the cadmium is more active than zinc when it reacts with oxygen [9]. With an increase in the Ar/O_2 gas ratios, the argon partial pressure is increased and the sputtering yield is enhanced, so the cadmium can react more easily with the oxygen. More cadmium atoms can replace zinc atoms and reach crystal lattice sites, thereby influencing on the surface chemistry. In addition, the different bonding states of the elements in the surface will result in a shift in the binding energy towards a lower value. A similar picture is observed when the dc power grows from 100 W to 150 W. In this case, an increase in deposition rate also takes place. Therefore, more cadmium atoms have a possibility to reach the growth interface and incorporate into ZnO matrix. It is confirmed by the largest intensity Cd-related XPS peaks for ZnCdO film deposited at the dc power of 150 W.

It should be also mentioned that the increasing of the Ar/O_2 ratio and dc power leads to the displacement of the Cd $3d_{5/2}$ peak toward the lower binding energy. This shift in the binding energy depends on the amount of Cd, thereby indicating an increase in number of new bonds (Cd–O–Zn and/or Cd–O–Cd) when the growth conditions were changed. Additionally, the integral area of the Cd $3d_{5/2}$ peak is also increased when the gas ratio and dc power are enhanced (as shown in Table I).

A surface stoichiometry of the grown films was evaluated by XPS. According to the rules of quantitative analysis of the XPS spectrum the relative atomic surface concentrations can be determined using the integrated area under principal peaks of Cd $3d_{5/2}$, Zn $2p_{3/2}$, and O $1s$ and a formula for quantification [10]:

$$C_x = \frac{I_x/S_x}{\sum_{i=1} I_i/S_i},$$

where C_x is the atomic concentration of element x, I_x is the integral intensity in the XPS spectrum of element x and S_x is the relative sensitivity factor (the Scoefield factor, RSF) for the element x. In order to perform the quantitative elemental analysis, RSF's from handbooks are utilized [11]. For Zn $2p_{3/2}$ bonded to O, Zn–O, we used a RSF of $S_{\mathrm{Zn}} = 18.9$, while for Cd $3d_{5/2}$ bonded to oxygen, Cd–O, we utilized a RSF of $S_{\mathrm{Cd}} = 12$. We also used a RSF for O $1s$ of $S_{\mathrm{O}} = 2.93$. To determine the stoichiometry of the ZnCdO surface, the relative O/(Cd+Zn) atomic ratio was calculated (the amounts of O is reckoned on the resolved O $1s$ peak from the formal valence state O^{2-}). The detailed XPS data is given in Table II. From Table II, we can easily find the tremendous discrepancy of $Zn_{1-x}Cd_xO$ films prepared at the different gas ratio and dc power. The obvious deviations from the stoichiometric ratios of O/(Cd+Zn) of 1:1 reflect the presence of native defects or substitution mechanism during process of ternary alloy formation.

TABLE II

Results of quantitative analysis for $Zn_{1-x}Cd_xO$ ternary alloys deposited at the different grown conditions.

Conditions	Relative atomic concentration [%]			Stoichiometric ratio, O/(Zn+Cd)
	O	Zn	Cd	
2:1, 100	50	46	4	1
4:1, 100	49	46	5	0.96
2:1, 150	43	45	11	0.75

As shown in Table II, O/(Zn+Cd) ratio for $Zn_{1-x}Cd_xO$ film, grown at the Ar/O_2 ratio of 4:1, is approximately 0.96 due to a decrease of the amount of the oxygen radicals [12]. On the other hand, the stoichiometric ratio changed from 1 to 0.75 when the film was deposited at the dc power of 150 W, indicating that the $Zn_{1-x}Cd_xO$ film changed from O-rich to Zn(Cd)-rich. These results indicate that the chemical stoichiometry of $Zn_{1-x}Cd_xO$ film is deeply related to an amount of reactive oxygen during the deposition.

Figure 2 exhibits the valence band spectra of $Zn_{1-x}Cd_xO$ ternary alloys, which are grown at the different growth conditions. The deconvolution of the scanned spectra indicates that the spectra consist of three peaks at the binding energies of ≈ 6, 11, and 19 eV. The weak peaks around the Fermi level ($E_{\mathrm{F}} = 0$ eV) are estimated to be a kind of non-local state in the band gap possibly caused by defects. Additionally, the peak feature around the Fermi level may come from the nonbonding O $2p$ orbitals [13]. The peak at ≈ 6 eV (region A) involves the O $2p$ orbitals hybridized with Zn $4s$ and $4p$ ones [13]. The peak at ≈ 11 eV (region B) is attributed to the Zn $3d$ band. The slight peak at the energy of 19 eV (region C) comes from the O $2s$ states. The contribution of Cd $4d$-like states superimposes the Zn $3d$-like band, however some small contributions of the valence states of Cd should be also in other parts of the valence band. With increasing the argon pressure and dc power, the width of the Zn $3d$-like band also increases, which is associated with increase of the contribution of Cd $4d$-like states (Cd $4d_{5/2}$: BE = 10.7 eV; Cd $4d_{3/2}$: BE = 11.6 eV).

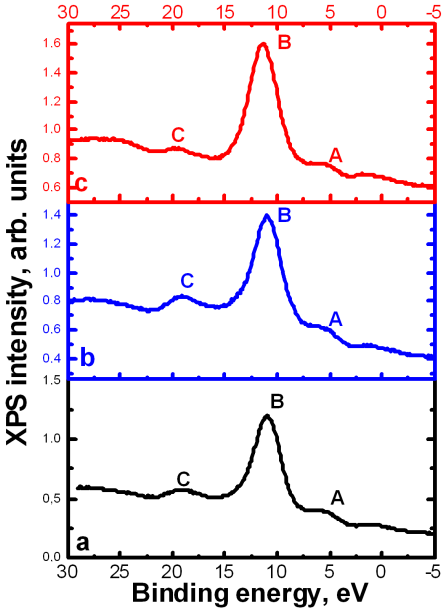

Fig. 2. XPS valence band spectra of the $Zn_{1-x}Cd_xO$ ternary alloys grown at the different growth conditions: a — Ar/O_2 gas ratio of 2:1, dc power of 100 W, b — 4:1, 100 W, c — 2:1, 150 W.

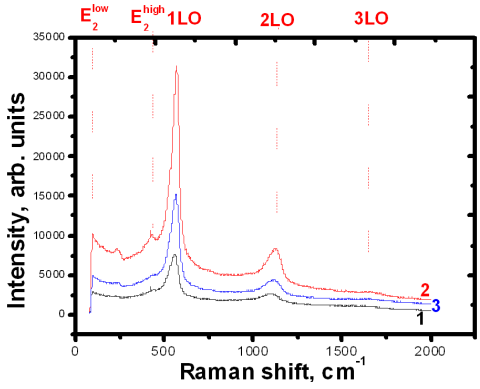

Fig. 3. Non-resonant Raman spectra of the $Zn_{1-x}Cd_xO$ ternary alloys, grown at the different growth conditions: Ar/O_2 gas ratio of 2:1, dc power of 100 W (curve 1); 4:1, 100 W (curve 2); 2:1, 150 W (curve 3).

Figure 3 depicts the non-resonant Raman spectra of the ZnCdO ternary alloys, grown at the different growth conditions. It should be noted that all spectra demonstrate the presence of two broad quasi-modes with mixed symmetry of $(A_1^{\mathrm{LO}} + E_1^{\mathrm{LO}})$. Their appearance is associated with the formation of the solid solution. On the

other hand, the LO phonon mode and its replicas may be associated with the presence of the oxygen vacancies and interstitial zinc or their complexes. It is well agreed with the XPS results, which revealed that the cadmium content may be increased via changing the growth parameters. More cadmium ions will lead to the activation of the additional amount of the defects, thereby enhancing the scattering cross-section of the defect-related LO phonon modes. Interestingly, the characteristic phonon modes of wurtzitic structure (E_2^{high} and E_2^{low}) are diminished. Nevertheless, we can observe that these modes become more distinguished and intensive after the gas ratio is increased from 2:1 to 4:1 (see in Fig. 3, curve 2). It should be mentioned that the E_2^{low} feature may be overlapped with an experimental artifact. Thus, it is difficult to find an unambiguous explanation for the effect of deposition parameters on the shape and position of the E_2^{low} mode.

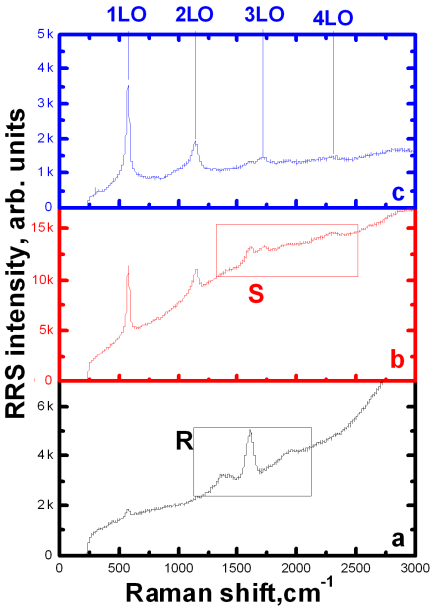

Fig. 4. Resonant Raman spectra of the $Zn_{1-x}Cd_xO$ ternary alloys, grown at the different growth conditions: Ar/O_2 gas ratio of 2:1, dc power of 100 W (a); 4:1, 100 W (b); 2:1, 150 W (c).

We have also studied the resonant Raman spectra for both samples (Fig. 4). The sample, grown at the gas ratio of 2:1 and dc power of 100 W, demonstrates the presence of the four peaks: 577, 1416, 1604, and 1992 cm^{-1}. Observed peaks (region R, Fig. 4) we cannot attribute to LO phonons of the ternary alloy with unchanged Cd content. It suggests that the composition fluctuations take place.

Increasing the gas ratio from 2:1 to 4:1 leads to an appearance of the sharp Raman peaks which can be attributed to the LO phonon modes. In this case, multiple scattering by the polar LO phonon is clearly observed up to the firth order in ZnCdO alloy. We also observe the additional peaks localized at the frequencies of 1616 cm^{-1} and 1990 cm^{-1} (region S, Fig. 4) and related to alloy

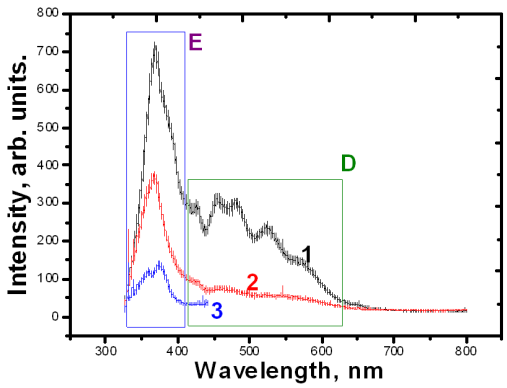

Fig. 5. PL spectra of the $Zn_{1-x}Cd_xO$ ternary alloys, grown at the different growth conditions: Ar/O_2 gas ratio of 2:1, dc power of 100 W (curve 1); 4:1, 100 W (curve 2); 2:1, 150 W (curve 3).

fluctuations or presence of second phases. The spectrum of the sample, deposited at the dc power of 150 W, consists of LO phonon band at 574 cm^{-1} and its overtones at the frequencies of 1141, 1716, 2294, and 2850 cm^{-1} (Fig. 4c). However, we can also see the additional modes at the 1592 and 1928 cm^{-1}, which are related to alloy fluctuations. It should be also noted that the 1LO mode of the sample, grown at the 150 W, red-shifted to the value of 574 cm^{-1} in comparison to that for one grown at the 100 W (577 cm^{-1}). It may be caused by the lattice expansion induced by Cd incorporation.

Figure 5 shows the PL spectra of the $Zn_{1-x}Cd_xO$ ternary alloys, grown at the different gas ratio of Ar/O_2 and the different dc power. Several significant features were found. First, all obtained spectra are characterized by the presence of the high-energy emission bands in the range of 363–369 nm (selected region E in Fig. 5). These bands are caused by the excitonic emission of pure ZnO. Second, ZnCdO phase with different cadmium content also contributes to the formation of the recombination channels. Especially, it is evidenced by the appearance of the shoulder in long-wavelength part of the ZnO-related emission band. Probably, we deal with the overlapping of the emission lines, which correspond to excitonic recombination in the regions with different cadmium content. Third, enhancing the gas ratio of Ar/O_2 from 2:1 to 4:1 leads to the disappearance of the broad developed PL band (region D in Fig. 5) associated with the superposition of the defect-related lines. It may be explained by the improvement of the crystallinity. An increase in dc power causes the significant diminishing of the PL intensity. It is related to enlargement of the concentration of the defects, which can play the roles of the nonradiative recombination centers. In this case, the cadmium content on the surface is largest (see XPS results).

4. Conclusions

$Zn_{1-x}Cd_xO$ ternary alloys were deposited by the dc magnetron sputtering method at the different growth

conditions (Ar/O_2 gas ratio and dc power). The elements present in the films were identified and their chemical states were also studied by means of the XPS measurements. The composition of the samples was calculated using the intensities of the Zn $2p_{3/2}$, Cd $3d_{5/2}$, and O $1s$ lines and the corresponding relative sensitivity factors. The shift in the binding energy values for all the peaks corresponding to Zn and O confirms the complete compound formation and the bonding with cadmium atoms. Mechanisms of the influence of the deposition conditions on the core and valence band spectra of the $Zn_{1-x}Cd_xO$ ternary alloys were proposed. The results of the Raman scattering and photoluminescence studies indicate the possibility to modify the phonon and emission spectra of the $Zn_{1-x}Cd_xO$ ternary alloys via changing the growth conditions.

References

[1] F. Ruske, C. Jacobs, V. Sittinger, B. Szyszka, W. Werner, *Thin Solid Films* **515**, 8695 (2007).

[2] Ya. Alivov, J.E. Van Nostrand, D.C. Look, M.V. Chukichev, *Appl. Phys. Lett.* **83**, 2943 (2003).

[3] G.V. Lashkarev, V.A. Karpyna, V.I. Lazorenko, A.I. Ievtushenko, I.I. Shtepliuk, V. Khranovskyy, *Low Temp. Phys.* **37**, 289 (2011).

[4] M. Lange, C.P. Dietrich, C. Czekalla, J. Zippel, G. Benndorf, M. Lorenz, J. Zuniga-Perez, M. Grundmann, *J. Appl. Phys.* **107**, 093530 (2010).

[5] T. Makino, C.H. Chia, N.T. Tuan, Y. Segawa, M. Kawasaki, A. Ohtomo, K. Tamura, H. Koinuma, *Appl. Phys. Lett.* **77**, 1632 (2000).

[6] T. Makino, Y. Segawa, M. Kawasaki, A. Ohtomo, R. Shiroki, K. Tamura, T. Yasuda, H. Koinuma, *Appl. Phys. Lett.* **78**, 1237 (2001).

[7] N.B. Chaure, Sh. Chaure, R.K. Pandey, *Solar Energy Mater. Solar Cells* **81**, 39 (2004).

[8] S. Sen, C.S. Liang, D.R. Rhiger, J.E. Stannard, H.F. Arlinghaus, *J. Electron. Mater.* **25**, 1188 (1996).

[9] I. Shtepliuk, G. Lashkarev, V. Khomyak, O. Lytvyn, P. Marianchuk, I. Timofeeva, A. Ievtushenko, V. Lazorenko, *Thin Solid Films* **520**, 4772 (2012).

[10] P. Bartolo-Perez, J.L. Pena, M.H. Farias, *Rev. Mex. Fis.* **44**, 9 (1998).

[11] J.F. Moulder, W.F. Stickle, P.E. Sobol, K.D. Bomben, *Handbook of X-ray Photoelectron Spectroscopy*, Eds. J. Chastain, R.C. King Jr., Physical Electronics, USA 1995.

[12] M. Furuta, T. Hiramatsu, T. Matsuda, C. Li, H. Furuta, T. Hirao, *J. Non-Cryst. Solids* **354**, 1926 (2008).

[13] M. Gabas, S. Gota, J.R. Ramos-Barrado, M. Sanchez, N.T. Barrett, J. Avila, M. Sacchi, *Appl. Phys. Lett.* **86**, 042104 (2005).